Nanoporous gold-based microbial biosensor for direct determination of sulfide

Zhuang Liu, Hanyue Ma, Huihui Sun, Rui Gao, Honglei Liu, Xia Wang, Ping Xu, Luying Xun

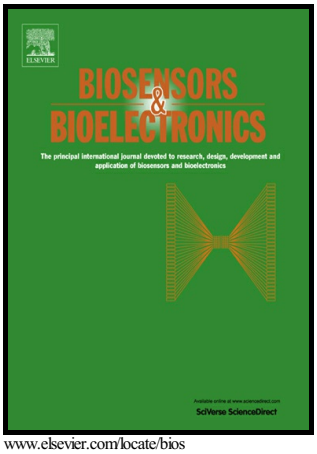

www.elsevier.com/locate/bios

PII: S0956-5663(17)30412-8
DOI: http://dx.doi.org/10.1016/j.bios.2017.06.037
Reference: BIOS9807

To appear in: *Biosensors and Bioelectronic*

Received date: 18 April 2017
Revised date: 7 June 2017
Accepted date: 18 June 2017

Cite this article as: Zhuang Liu, Hanyue Ma, Huihui Sun, Rui Gao, Honglei Liu Xia Wang, Ping Xu and Luying Xun, Nanoporous gold-based microbia biosensor for direct determination of sulfide, *Biosensors and Bioelectronic* http://dx.doi.org/10.1016/j.bios.2017.06.037

Nanoporous gold-based microbial biosensor for direct determination of sulfide

Zhuang Liu, Hanyue Ma, Huihui Sun, Rui Gao, Honglei Liu, Xia Wang*, Ping Xu[1], Luying Xun

State Key Laboratory of Microbial Technology, Shandong University, Jinan 250100, P. R. China

*Corresponding author. Prof. Xia Wang, Tel/Fax: +86-531-88366231. E-mail: ghwx@sdu.edu.cn

[1] *Present address: Key Laboratory of Microbial Metabolism and School of Life Sciences and Biotechnology, Shanghai Jiao Tong University, Shanghai 200240, P. R. China*

ABSTRACT

Environmental pollution caused by sulfide compounds has become a major problem for public health. Hence, there is an urgent need to explore a sensitive, selective, and simple sulfide detection method for environmental monitoring and protection. Here, a novel microbial biosensor was developed using recombinant *Escherichia coli* BL21 (*E. coli* BL21) expressing sulfide:quinone oxidoreductase (SQR) for sulfide detection. As an important enzyme involved in the initial step of sulfide metabolism, SQR oxidizes sulfides to polysulfides and transfers electrons to the electron transport chain. Nanoporous gold (NPG) with its unique properties was selected for recombinant *E. coli* BL21 cells immobilization, and then glassy carbon electrode (GCE) was modified by the resulting *E. coli*/NPG biocomposites to construct an *E. coli*/NPG/GCE bioelectrode. Due to the catalytic oxidation properties of NPG for sulfide, the electrochemical reaction of the *E. coli*/NPG/GCE bioelectrode is attributed to the co-catalysis of SQR and NPG. For sulfide detection, the *E. coli*/NPG/GCE bioelectrode showed a good linear response ranging from 50 μM to 5 mM, with a high sensitivity of 18.35 $\mu A \cdot mM^{-1} \cdot cm^{-2}$ and a low detection limit of 2.55 μM. The anti-interference ability of the *E. coli*/NPG/GCE bioelectrode is better than that of enzyme-based inhibitive biosensors. Further, the *E. coli*/NPG/GCE bioelecrode was successfully applied to the detection of sulfide in wastewater. These unique properties potentially make the *E. coli*/NPG/GCE bioelectrode an excellent choice for reliable sulfide detection.

Keywords: sulfide:quinone oxidoreductase; nanoporous gold; recombinant *E. coli* BL21; microbial biosensor; sulfide

1. Introduction

Sulfide compounds (H_2S, HS^-, and S^{2-}) are versatile reagents that are used in many industries, such as petrochemical, textile, refinery, and oil industries (Colon et al., 2008; Liu et al., 2008; Ebrahimi et al., 2014). Recently, environmental pollution caused by sulfide has become a major problem for public health. For example, hydrogen sulfide is a toxic, flammable, and colorless gas (Syed et al., 2006). At low concentrations (15–50 ppm), H_2S can cause headache, eye irritation, and dizziness (Milby and Baselt, 1999; Ma et al., 2006; Syed et al., 2006). Moreover, H_2S may have an anesthetic effect, and a several-minute exposure to greater than 700 ppm may lead to death (Syed et al., 2006; Colon et al., 2008; Rattanapan et al., 2009). Thus, it is necessary to control sulfide even at low concentrations in the environment. Additionally, increasing evidence shows that endogenous sulfide is a gas transmitter (alongside nitric oxide and carbon monoxide) and could play a significant role in mammalian tissues and cells (Li et al., 2012). Monitoring endogenous sulfide concentration in patients has great significance for guiding clinical treatment. Therefore, a sensitive, selective, and simple method for sulfide detection is urgently needed to both monitor environmental pollution and detect endogenous sulfides.

Various methods for sulfide detection have been reported, such as spectrophotometry (Davidson et al., 2009), fluorimetry (Yang et al., 2009), electrogenerated chemiluminescence (Huang et al., 2007), inductively coupled plasma-atomic emission spectrometry (Colon et al., 2008), chromatography (Kolotilina and Dolgonosov, 2005), atomic absorption spectroscopy (Afkhami and

Khalafi, 2005), and biosensors (Janfada et al., 2015; Xu et al., 2016). Among these techniques, biosensors have attracted wide attention given their unique advantages such as high selectivity and sensitivity, easy operation, fast response, and real-time analysis (Gomathi et al., 2011; Ebrahimi et al., 2014; Gao et al., 2014; Poor et al., 2014). In general, there are two kinds of representative biosensors for sulfide detection. Firstly, inhibitive biosensors were based on the inhibition of enzyme activity caused by sulfide exposure (Shan et al., 2010; Savizi et al., 2012). The enzymes commonly used in inhibitive biosensors were horseradish peroxidase (HRP) (Liu et al., 2008), peroxidase (Savizi et al., 2012; Kariminia et al., 2013), cytochrome C oxidase (Albery et al., 1990), and ascorbate oxidase (Ebrahimi et al., 2014). Second, microbial biosensors used microorganisms as biological recognition elements that to directly oxidize sulfides. For example, *Thiobacillus thioparus* was used to fabricate a biosensor for sulfide detection (Ebrahimi et al., 2014; Mirzaei et al., 2014; Qi et al., 2014). Janfada et al. (2015) constructed a hydrogen sulfide biosensing system with four sulfur-oxidizing bacteria. However, these two types of biosensors have some limitations for sulfide detection. For inhibitive biosensors, their anti-interference ability was poor due to the potential presence of many other inhibitors such as cyanide and/or azide ions (Xu et al., 2016). For microbial biosensors, sulfur-oxidizing bacteria usually require a very complex culture condition (Janfada et al., 2015), and the oxidation rate of sulfides is slow given the low-level expression of the enzymes involved in sulfide biodegradation. Therefore, investigation into biosensors that possess a high catalytic activity, high selectivity, and good anti-interference ability for

sulfide detection remains a priority in the field.

Sulfide:quinone oxidoreductase (SQR) is an ancient flavoprotein in disulfide oxidoreductase family, which plays an important role in sulfide metabolism and maintaining sulfide homeostasis (Zhang et al., 2016). SQR can oxidizes sulfide to elemental sulfur, polysulfide, or octasulfur rings, and transfers two electrons via the FAD cofactor to the quinone pool in the cell membrane (Zhang et al., 2014; Zhang et al., 2016). Further, SQR possesses high catalytic activity (Zhang et al., 2016), which could make it a good choice as a recognition element for sulfide detection. However, the expression level of SQR in bacterial strains is generally poor, and this remains the major limitation in the construction of a microbial biosensor. Recombinant bacteria with over-expressed SQR may solve this limitation (Prathap et al., 2012).

The maintenance of microbial activity is another challenge in microbial biosensor construction. The immobilization of bio-recognition element plays a significant role in a biosensor construction, which could influence the electrochemical activity, stability, and reproducibility of a biosensor (Mirzaei et al., 2014; Hao et al., 2017). Recently, three-dimensional nanomaterials with higher strength-to-weight and surface-area-to-volume ratios have been considered as the ideal choices for the bio-recognition element immobilization (Ding and Chen, 2009; Du et al., 2016). As one of three-dimensional nanomaterials, nanoporous gold (NPG) with tunable porosity, excellent electrochemical properties, and high biocompatibility has aroused attention in the fabrication of biosensors and in the immobilization of enzymes (Ding and Chen, 2009; Wang et al., 2011; Yan et al., 2012; Wu et al., 2014). When NPG

served as a support, the strong gold-sulfur covalent interactions make the immobilization of enzymes or microbial cells more stable in practical application (Wang et al., 2011; Wu et al., 2014). In our previous work, enzyme-NPG biocomposites were successfully established by assembling various enzymes (such as lipase, catalase, and HRP) on the surface of NPG, which exhibited remarkable catalytic abilities and stabilities (Wang et al., 2011). Then, we constructed lipase/NPG, glucose oxidase (GOx)/NPG, and HRP/NPG biosensors. These biosensors performed well in the detection of triglycerides, glucose, phenols, and aromatic amines (Wu et al., 2014; Wu et al., 2015; Wu et al., 2016). Hence, we supposed that the microorganisms/NPG biocomposites could also perform very well for the detection or biodegradation of sulfide.

In this work, a recombinant *E. coli* BL21 strain over-expressing SQR on cell membranes was constructed for sulfide detection. NPG was selected for the immobilization of recombinant *E. coli* BL21 cells, and glassy carbon electrodes (GCEs) were modified with these microorganisms/NPG biocomposites to produce the *E. coli*/NPG/GCE bioelectrode. The electrochemical behavior, anti-interference ability, stability, reproducibility, and practical performance of the *E. coli*/NPG/GCE bioelectrode were evaluated in detail.

2. Experimental Methods

Sulfide microbial biosensor design and measurement

NPG was made by dealloying method (Wang et al., 2011). A recombinant *E. coli* BL21 (DE3) strain overexpressing SQR was constructed and immobilized on NPG to

fabricate an *E. coli*/NPG biocomposite. GCE was modified with the *E. coli*/NPG biocomposites to produce an *E. coli*/NPG/GCE bioelectrode. The details of the fabricated method of NPG, the cloning, overexpression, cell culture, and immobilization of recombinant *E. coli* BL21, and the construction of NPG/GCE electrode, HRP/NPG/GCE, *E. coli*/NPG/GCE, and *E. coli*/HRP/NPG/GCE bioelectrode were described in the Supporting Information. All electrochemical measurements were performed in a three-electrode cell at room temperature. Sulfide detection and real samples analysis were described in detail in the Supporting Information.

3. Results and discussion

3.1. The overexpression of SQR

To verify the cloning of Cp*sqr* in *E. coli* BL21 cells, polymerase chain reaction (PCR) and restriction endonuclease digestion were performed using recombinant plasmids isolated from transformants. As shown in Fig. 1A, the restriction endonuclease digestion of pET30-SQR with NdeI and XhoI yielded a 1.2 kb Cp*sqr* insert and a 5.44 kb pET30 Ec/Lic vector (lane 2). The yielded 1.2 kb Cp*sqr* gene (Fig. 1A, lane 2) was consistent with the PCR products (Fig. 1A, lane 3) in size, which was synthesized by using recombinant pET30-SQR as a template. Further, the restriction endonuclease digestion of plasmid pET30 with NdeI and XhoI yielded an expected product of 5.44 kb (Fig. 1A, lane 4), which was also consistent with the pET30 Ec/Lic vector in size (Fig. 1A, lane 2). These results indicated that Cp*sqr* was successfully cloned into *E. coli* BL21 cells.

To confirm Cp*sqr* gene expression in *E. coli* BL21 cells, sodium dodecyl sulfate polyacrylamide gel electrophoresis (SDS-PAGE) was carried out (Fig. 1B). Compared to the control without isopropyl-1-thio-b-D-galactopyranoside (IPTG) induction (Fig. 1B, lane 1), the recombinant *E. coli* BL21 cells could produce high amounts of SQR protein after 3 h and 6 h of IPTG induction (Fig. 1B, lanes 2 and 3). The recombinant SQR protein matched the calculated molecular mass (~50 kDa) of the SQR protein from *Cupriavidus pinatubonensis* JMP134 (Fig. 1B). These results demonstrated that the Cp*sqr* gene was successfully expressed in *E. coli* BL21 cells.

To further examine the expression level of SQR in recombinant *E. coli* BL21 cells, the methylene blue spectrophotometric method was used to determine the catalytic oxidation of sulfide by the recombinant *E. coli* BL21 cells (Fig. 2A). Within 2 min of reaction initiation, the concentration of sulfide had sharply declined from 24.81 μM to 3.66 μM. After 4 min, the concentration of sulfide had decreased to 1.91 μM (Fig. 2A). Fig. 2B-a, 2B-b, and 2B-c are relative to the reactive state of 0, 2, and 4 min in Fig. 2A, respectively. The concentration of sulfide corresponds to the color of the reaction solution as shown in Fig. 2B. As the reaction time increased, the color of the reaction solution gradually changed from blue to pink (from Fig. 2B-a to Fig. 2B-c). These results demonstrated that SQR was successfully expressed in recombinant *E. coli* BL21 cells, and was highly active in oxidizing sulfides. Additionally, it is important to note that *E. coli* BL21 strain is a low-cost, rapid breeding, and thoroughly studied bacterium, which may be beneficial to large-scale applications. Moreover, the recombinant *E. coli* BL21 over-expressing SQR does not require complex culture

conditions compared to sulfur-oxidizing bacteria (Janfada et al., 2015). Therefore, the recombinant *E. coli* BL21 over-expressing SQR was suitable for the fabrication of a microbial biosensor for sulfide detection.

3.2. Construction and characterization of the E. coli/NPG/GCE bioelectrode

After SQR successfully expressed in *E. coli* BL21 cells, NPG was selected to immobilize recombinant *E. coli* BL21 cells and thereby construct an *E. coli*/NPG biocomposite. GCEs were then modified by the resulting *E. coli*/NPG biocomposite to fabricate an *E. coli*/NPG/GCE bioelectrode. The morphology of NPG and *E. coli*/NPG biocomposites were characterized by scanning electron microscope (SEM). As shown in Fig. 3A, NPG has a pore size of ca. 35 nm. In contrast, the recombinant *E. coli* BL21 cells on the NPG surface were approximately 2 μm in length and 0.8 μm in diameter (Fig. 3B). Evidently, the recombinant *E. coli* BL21 cells were larger than the pore of NPG in size (Fig. 3B). Additionally, NPG has an open bicontinuous nanoporous structure and high surface area (Fig. 3A), which could increase the adhesion of *E. coli* BL21 cells on NPG and facilitate sufficient substrate and electron transfer. Further, SQR with sulfhydryl (-SH) groups could combine with active gold atoms to form strong gold-sulfur covalent interactions (Wang et al., 2011), which makes the attachments of *E. coli* BL21 cells on the NPG surface more firm and stable.

3.3. Electrochemical behavior of E. coli/NPG/GCE bioelectrode

The electrochemical behaviors of NPG/GCE electrode and *E. coli*/NPG/GCE bioelectrode were tested in 15 ml deaerated phosphate buffer solution (PBS, 50 mM, pH 7.5) using cyclic voltammetry (CV) technique at a scan rate of 50 $mV \cdot s^{-1}$. As

shown in Fig. 4A, it was clear that the redox peak current densities of the *E. coli*/NPG/GCE bioelectrode were both lower than that of the NPG/GCE electrode. For the *E. coli*/NPG/GCE bioelectrode, *E. coli* BL21 cells were insulated and acted as resistance, which lowered the current response. These results also indicated that *E. coli* BL21 cells were successfully immobilized onto the NPG/GCE electrode.

Fig. 4B showed the CVs of the *E. coli*/NPG/GCE bioelectrode in 15 ml deaerated PBS (50 mM, pH 7.5) at different scan rates. Within the scanning potential range of -0.7 ~ +1.2 V, a couple of asymmetrical redox peaks were obtained from the cyclic voltammograms. Moreover, with the increase in scan rate, both the redox peak currents and redox potential were affected. The oxidation peak potential (E_{pa}) positively shifted from 0.882 V at 10 $mV \cdot s^{-1}$ to 1.134 V at 1000 $mV \cdot s^{-1}$, and the reduction peak potential (E_{pc}) negatively shifted from 0.446 V at 10 $mV \cdot s^{-1}$ to 0.269 V at 1000 $mV \cdot s^{-1}$, which demonstrated that the electrode reaction gradually became more irreversible. The peak current densities of the redox peaks were positively associated with the scan rates. As shown in the inset of Fig. 4B, the peak current density was linearly correlated with the square root of the scan rate; the correlation coefficients for cathodic and anodic peaks being 0.9987 and 0.9976, respectively. These results indicated that the electrochemical reaction of sulfide on the surface of the *E. coli*/NPG/GCE bioelectrode was a diffusion-controlled, quasi-reversible process, which is consistent with previously reported results (Li et al., 2015; Du et al., 2016; Wu et al., 2016; Chen et al., 2017).

To explore the function of the *E. coli*/NPG/GCE bioelectrode during the

electrochemical oxidation of sulfide, the NPG/GCE electrode and the *E. coli*/NPG/GCE bioelectrode were compared in deaerated PBS (50 mM, pH 7.5) in the presence of 4 mM Na_2S using differential pulse voltammetry (DPV) technique. Fig. 4C showed that both NPG/GCE electrode and *E. coli*/NPG/GCE bioelectrode had the ability to oxidize sulfide. However, the peak current density of the *E. coli*/NPG/GCE bioelectrode was higher than that of the NPG/GCE electrode at the potential of -0.22 V. To further confirm the function of recombinant *E. coli* BL21 over-expressing SQR for sulfide oxidation, an HRP/NPG/GCE bioelectrode and an *E. coli*/HRP/NPG/GCE bioelectrode were compared in deaerated PBS (50 mM, pH 7.5) in the presence of 4 mM Na_2S using the DPV technique. As shown in Fig. 4C, the HRP/NPG/GCE bioelectrode showed no electrocatalytic activity for sulfide. In contrast, an obvious oxidation peak current response for the *E. coli*/HRP/NPG/GCE bioelectrode was observed at -0.22 V, indicating that recombinant *E. coli* BL21 over-expressing SQR played an important role in sulfide electrochemical oxidation. These results demonstrated that the electrochemical reaction on the *E. coli*/NPG/GCE bioelectrode was attributed to the co-catalysis of SQR and NPG.

To investigate the sulfide oxidation reaction kinetics on the surface of the *E. coli*/NPG/GCE bioelectrode, the *E. coli*/NPG/GCE bioelectrode was further explored by the CV method in PBS (50 mM, pH 7.5) containing sulfide (2 mM) at different scan rates. As shown in Fig 4D, a single oxidation peak emerged around -0.15 V in the presence of sulfides. Furthermore, the sulfide oxidation peak potential positively shifted from -0.172 V at 10 $mV \cdot s^{-1}$ to -0.1102 V at 200 $mV \cdot s^{-1}$, which is evidence for

this process being irreversible (Jin et al., 2014). As shown in the inset of Fig. 4D, a perfect linear relationship between the peak current density and the scan rate from 10 $mV \cdot s^{-1}$ to 200 $mV \cdot s^{-1}$ was obtained with a regression coefficient of 0.999. These characteristics confirmed that the electron transfer process in the presence of sulfide was a diffusion-controlled, irreversible process, which agrees well with other reports (Yang, et al., 2009; Qi et al., 2014).

It has been reported that nanostructured gold, such as Au nanoclusters (Yang et al., 2009), Au and Pt nanoparticles (Vallejos et al., 2015), and Ag-Au nanoalloys (Chang et al., 2016), could catalyze the oxidation of sulfide. In this work, we found that NPG could achieve selective oxidation of sulfides at a lower potential of -0.22 V. According to Alfonso (2008), when sulfide (the main form in PBS is HS^-) oxidation is performed on the NPG/GCE electrode, the sulfides might be absorbed onto the surface of the NPG by Au-S bonds and then oxidized to elemental sulfur. The working principle of NPG during the electrochemical catalysis of sulfide could be expressed as follows:

$$HS^-(S^{2-}, H_2S) \xrightarrow{NPG} S^0 + 2e^- \quad (1)$$

The working principle of recombinant *E. coli* BL21 over-expressing SQR during the electrochemical catalysis of sulfide could be expressed as follows:

$$HS^-(S^{2-}, H_2S) + SQR_{ox}(FAD) + 2H^+ \rightarrow S^0(polysulfide) + SQR_{red}(FADH_2) \quad (2)$$

$$SQR_{red}(FADH_2) + Q \rightarrow SQR_{ox}(FAD) + QH_2 \quad (3)$$

$$QH_2 \xrightarrow{Bioelectrode} Q + 2e^- + 2H^+ \quad (4)$$

According to Griesbeck et al. (2002) and Zhang et al. (2015), SQR could catalyze the oxidation of sulfide and the reduction of ubiquinone (Q). In this process, two electrons

were transferred from a sulfide ion to an FAD cofactor to form $FADH_2$, and SQR was changed from an oxidized state (SQR_{ox}) to a reduced state (SQR_{red}). Then $FADH_2$ was oxidized to FAD by transferring two electrons to the Q to form dihydroubiquinone (QH_2). The SQR_{red} was oxidized to its original form of SQR_{ox}. In addition, the Q/QH_2 couple is one of the typical quinone compounds that can act as a good electron mediator in an electrochemical reaction (Qiu et al., 2012; Wu et al., 2016). In this study, QH_2 was subsequently reduced back to Q by the bioelectrode as described in Equation (4). Therefore, the electrochemical oxidation of sulfide on the *E. coli*/NPG/GCE bioelectrode was completed by the contribution of both SQR and NPG as shown in Fig. 3C. The current response of the *E. coli*/NPG biocomposite was higher than that of SQR or NPG alone (Fig. 4C), which also confirmed that the electrochemical reaction of sulfide on the *E. coli*/NPG/GCE bioelectrode was attributed to the co-catalysis of SQR and NPG. Thus, sulfide detection can be achieved by detecting the changes in the oxidation peak current density using the *E. coli*/NPG/GCE bioelectrode.

3.4. Sulfide detection by E. coli/NPG/GCE bioelectrode

To evaluate the electrochemical performances of the *E. coli*/NPG/GCE bioelectrode, a range of sulfide concentrations were investigated using the DPV technique in deaerated PBS (50 mM, pH 7.5). With increasing sulfide concentration, the peak current density increased at the potential of -0.22 V (Fig. 5A). The inset profiles in Fig. 5A showed that the peak current densities were linearly associated with the sulfide concentration when the concentration ranged from 50 μM to 5 mM

(correlation coefficient of 0.9898). The linear regression equations for sulfide concentration were determined to be $j\ (\mu A\ cm^{-2}) = 2.59505 + 0.01835 \times C_{sulfide}(\mu M)$. In addition to the wide linear range, the *E. coli*/NPG/GCE bioelectrode had a high sensitivity of 18.35 $\mu A \cdot mM^{-1} \cdot cm^{-2}$ and a low detection limit of 2.55 μM (S/N=3). The relative standard deviation (RSD) for determining of sulfide was 2.78% (n=5). The low RSD indicated that sulfide measurements using the *E. coli*/NPG/GCE bioelectrode were highly reproducible. These results indicated that the *E. coli*/NPG/GCE bioelectrode presented a larger linear range, higher sensitivity, and lower detection limit than other electrochemical systems for sulfide detection (Table S1).

3.5. Selectivity and anti-interference of E. coli/NPG/GCE bioelectrode

Selectivity and anti-interference are critical factors for a biosensor, as the biosensor needs to specifically recognize a target substrate in practical applications. To evaluate the anti-interference of *E. coli*/NPG/GCE bioelectrode, cations, anions, and organic pollutants were added separately into deaerated PBS (50 mM, pH 7.5) containing sulfide. Obviously, the cations (Fig. 5B) and anions (Fig. 5C) mentioned above exhibited negligible interference on sulfide detection using the *E. coli*/NPG/GCE bioelectrode. These results differed from previous reports where cyanide (CN^-) and some other ions interfered significantly with sulfide detection using an enzyme-based inhibitive biosensor (Zhao et al., 1996; Sun et al., 2016). For example, an inhibitive biosensor based on an HRP-colloidal gold developed by Zhao et al. (1996) was more sensitive to CN^- and thiourea than sulfide. In our previous

work, CN^- interfered greatly with sulfide detection using an amperometric inhibitive biosensor based on an HRP-NPG biocomposite (Sun et al., 2016). In contrast, CN^- showed negligible changes (0.76%) on peak current signal during sulfide detection using the *E. coli*/NPG/GCE bioelectrode (Fig. 5C). Further, organic sulfide and other organic pollutants also showed small or no changes on peak current signal during sulfide detection and the relative peek current density was < 5% (Fig. 5D). These results indicated that the *E. coli*/NPG/GCE bioelectrode presented better anti-interference properties than some biosensors reported previously for sulfide detection (Zhao et al., 1996; Liu et al., 2008; Sun et al., 2016).

3.6. Stability of E. coli/NPG/GCE bioelectrode

Stability is a basic requirement for a microbial biosensor. To assess the stability of the *E. coli*/NPG/GCE bioelectrode, it was preserved in a culture solution at 4^{o}C and then was measured against 500 μM sulfide every seven days. The electrochemical current signal exhibited no changes over a period of seven days. After 28 days of storage, the *E. coli*/NPG/GCE bioelectrode retained 96.35% of its original current response. These results confirmed that the *E. coli*/NPG/GCE bioelectrode exhibited excellent stability, and this was likely due to NPG's excellent biocompatibility and active surface (Wang et al., 2011; Wu et al., 2014, 2015, 2016), which are very important for microbial cell immobilization.

3.7. Sulfide detection in wastewater

To investigate the practical performance of *E. coli*/NPG/GCE bioelectrodes, two types of wastewater samples were analyzed. Firstly, wastewater provided by Jining

wastewater treatment plant (China) was analyzed by the *E. coli*/NPG/GCE bioelectrode and the methylene blue spectrophotometric method, respectively. As shown in Table 1, the deviation rate was only +2.15%, demonstrating that there is no significant difference between the two detection methods. Second, a synthetic wastewater sample containing 5 ml wastewater mentioned above and 10 ml PBS (50 mM, pH 7.5) were analyzed using the *E. coli*/NPG/GCE bioelectrode. Prior to analysis, a certain amount of sulfide was added to the synthetic wastewater samples. Meanwhile, these synthetic wastewater samples were also measured by the methylene blue spectrophotometric method. The average recovery and deviation rate were 102.89% and +2.89% respectively, indicating that the *E. coli*/NPG/GCE bioelectrode was practical and accurate for sulfide detection in actual wastewater samples.

4. Conclusion

In conclusion, a novel NPG-based microbial biosensor was developed for direct sulfide detection using recombinant *E. coli* BL21 over-expressing SQR. The resulting *E. coli*/NPG/GCE bioelectrode achieved selective oxidation of sulfides due to the co-catalysis of SQR and NPG. Moreover, the *E. coli*/NPG/GCE bioelectrode showed a good linear relationship between peak current density and sulfide concentration in a wide detection range (50 μM–5 mM) with a high sensitivity of 18.35 $\mu A \cdot mM^{-1} \cdot cm^{-2}$ and a low detection limit of 2.55 μM. The anti-interference properties of the *E. coli*/NPG/GCE bioelectrode were better than that of enzyme-based inhibitive biosensors. As evidence for its potential practical application, sulfides were successfully detected using the *E. coli*/NPG/GCE bioelectrode. Therefore, the *E.*

coli/NPG/GCE bioelectrode with wide detection range, high sensitivity, excellent anti-interference, and good stability could be an excellent choice for sulfide detection.

Acknowledgments

This work was supported by grants from the National Natural Science Foundation of China (31570103 and 21177074), Shandong Science & Technology Fund Planning Project (2014GSF117021), and The Fundamental Research Funds of Shandong University (2017JC024).

References

Afkhami, A., Khalafi, L., 2005. Microchim. Acta 150, 43-46.

Albery, W.J., Cass, A.E.G., Mangold, B.P., Shu, Z.X., 1990. Biosens. Bioelectron. 5, 397-413.

Alfonso, D.R., 2008. Surf. Sci. 602, 2758-2768.

Chang, L., Fisher, A., Liu, Z.P., Cheng, D.J., 2016. RCS Adv. 6, 16285-16291.

Chen, X.L., Yang, G.M., Feng, S.P., Shi, L., Huang, Z.L., Pan, H.B., Liu, W., 2017. Appl. Surf. Sci. 402, 232-244.

Colon, M., Todolí, J.L., Hidalgo, M., Iglesias, M., 2008. Anal. Chim. Acta 609, 160-168.

Davidson, J.M., Pikramenou, Z., Ponce, A., Winpenny, R.E.P., 2009. Anal. Chem. 81, 3669-3675.

Ding, Y., Chen, M.W., 2009. MRS Bull. 34, 569-576.

Du, X.J., Jiang, D., Hao, N., Qian, J., Dai, L., Zhou, L., Hu, J., Wang, K., 2016, Anal. Chem. 88, 9622-9629.

Ebrahimi, E., Yazdian, F., Amoabediny, G., Shariati, M.R., Janfada, B., Saber, M., 2014. Process Biochem. 49, 1393-1401.

Gao, Y.F., Yang, T., Yang, X.L., Zhang, Y.S., Xiao, B.L., Hong, J., Sheibani, N., Ghourchian, H., Hong, T., Moosavi-Movahedi, A.A., 2014. Biosens. Bioelectron. 60, 30-34.

Ghadiri, M., Kariminia, H.R., Azad, R.R., 2013. Ecotoxicol. Environ. Saf. 91, 117-121.

Gomathi, P., Ragupathy, D., Choi, J.H., Yeum, J.H., Lee, S.C., Kim, J.C., Lee, S.H., Do Ghim, H., 2011. Sens. Actuators, B 153, 44-49.

Griesbeck, C., Schütz, M., Schödl, T., Bathe, S., Nausch, L., Mederer, N., Vielreicher, M., Hauska, G., 2002. Biochemistry 41, 11552-11565.

Hao, N., Zhang, X., Zhou, Z., Qian, J., Liu, Q., Chen, S.B., Zhang, Y., Wang, K., 2017, Sensor. Actuat. B 250, 476-483.

Huang, R.F., Zheng, X.W., Qu, Y.J., 2007. Anal. Chim. Acta 582, 267-274.

Janfada, B., Yazdian, F., Amoabediny, G., Rahaie, M., 2015. Biotechnol. Appl. Biochem. 62, 349-356.

Jin, W., Wu, G.S., Chen, A.C., 2014. Analyst 139, 235-241.

Kolotilina, N.K., Dolgonosov, A.M., 2005. J. Anal. Chem. 60, 738-742.

Li, G.F., Luo, H.K., Li, L.F., Zhang, Q.Z., Xie, L.J., Jiang, H., Li, L.P., Hao, N., Wang, W.W., Zhang, J.X., 2012. Clin. Exp. Pharmacol. Physiol. 39, 765-771.

Li, L.L., Wang, Y.Q., Pan, L.J., Shi, Y., Cheng, W., Shi, Y., Yu, G.H., 2015. Nano Lett. 15, 1146-1151.

Liu, L.J., Chen, Z.C, Yang, S.M., Jin, X., Lin, X.F., 2008. Sens. Actuators, B 129, 218-224.

Ma, Y.L., Zhao, J.L., Yang, B.L., 2006. Int. Biodeterior. Biodegrad. 57, 93-98.

Milby, T.H., Baselt, R.C., 1999. Am. J. Ind. Med. 35, 192-195.

Mirzaei, M., Amoabediny, G., Yazdian, F., Sheikhpour, M., Ebrahimi, E., Zadeh, B.E.H., 2014. Process Biochem. 49, 380-385.

Poor, N.Z.M., Baniasadi, L., Omidi, M., Amoabediny, G., Yazdian, F., Attar, H., Heydarzadeh, A., Zarami, A.S.H., Sheikhha, M.H., 2014. Enzyme Microb. Tech. 63, 7-12.

Prathap, M.U.A., Chaurasia, A.K., Sawant, S.N., Apte, S.K., 2012. Anal. Chem. 84, 6672-6678.

Qi, P., Zhang, D., Wan, Y., 2014. Electroanalysis. 26, 1824-1830.

Qiu, C.C., Wang, X., Liu, X.Y., Hou, S.F., Ma, H.Y., 2012. Electrochim. Acta 67, 140-146

Rattanapan, C., Boonsawang, P., Kantachote, D., 2009. Bioresour. Technol. 100, 125-130.

Savizi, I.S.P., Kariminia, H.R., Ghadiri, M., Roosta-Azad, R., 2012. Biosens. Bioelectron. 35, 297-301.

Shan, D., Li, Q.B., Ding, S.N., Xu, J.Q., Cosnier, S., Xue, H.G., 2010. Biosens. Bioelectron. 26, 536-541.

Sun, H.H., Liu, Z., Wu, C., Xu, P., Wang, X., 2016. Sci. Rep. 6, 30905.

Suprun, E.V., Budnikov, H.C., Evtugyn, G.A., Brainina, K.Z., 2004. Bioelectrochem. 63, 281-284.

Syed, M., Soreanu, G., Falletta, P., Béland, M., 2006. Can. Biosyst. Eng. 48, 1-14.

Vallejos, S., Gracia, I., Bravo, J., Figueras, E., Hubalek, J., Cane, C., 2015. Talanta 139, 27-34.

Vosoughi, A., Yazdian, F., Amoabediny, G., Hakim, M., 2015. Biosens. Bioelectron. 70, 106-114.

Wang, X., Liu, X.Y., Yan, X.L., Zhao, P., Ding, Y., Xu, P., 2011. PLoS One 6, e24207.

Wu, C., Liu, X.Y., Li, Y.F., Du, X.Y., Wang, X., Xu, P., 2014. Biosens. Bioelectron. 53, 26-30.

Wu, C., Liu, Z., Sun, H.H., Wang, X., Xu, P., 2016. Biosens. Bioelectron. 79, 843-849.

Wu, C., Sun, H.H., Li, Y.F., Liu, X.Y., Du, X.Y., Wang, X., Xu, P., 2015. Biosens. Bioelectron. 66, 350-355.

Xu, T.L., Scafa, N., Xu, L.P., Zhou, S.F., Al-Ghanem, K.A., Mahboob, S., Fugetsu, B., Zhang, X.J., 2016. Analyst. 141, 1185-1195.

Yang, B., Wang, S.Q., Tian, S.B., Liu, L.Z., 2009. Electrochem. Commun. 11, 1230-1233.

Yan, X.L., Meng, F.H., Xie, Y., Liu, J.G., Ding, Y., 2012. Sci. Rep. 2, 941.

Yang, X.F., Wang, L.P., Xu, H.M., Zhao, M.L., 2009. Anal. Chim. Acta 631, 91-95.

Zhang, Y.F., Qadri, A., Weiner, J.H., 2016. Biochem. Cell Biol. 94, 159-166.

Zhang, Y.F., Weiner, J.H., 2014. Arch. Biochem. Biophys. 564, 110-119.

Zhao, J.G., Henkens, R.W., Crumbliss, A.L., 1996. Biotechnol. Prog. 12, 703-708.

Table 1 Determination of sulfide in wastewater samples.

Sample	Added concentration (μM)	Proposed biosensor (μM)	Standard spectrophotometric method (μM)	Recovery (%)	Deviation rate (%)
Wastewater	-	56.95 ± 1.05	55.75 ± 1.54	-	+2.15
Synthetic wastewater	700	742.10 ± 5.94	718.58 ± 6.86	103.27	+3.27
Synthetic wastewater	1300	1351.65 ± 8.98	1318.58 ± 10.42	102.51	+2.51

Figure legends:

Fig. 1. The cloning and overexpression of SQR in recombinant *E. coli* BL21 cells. (A) The cloning of Cp*sqr* gene into pET30 Ec/Lic vector. Various lanes show the following: 1 kb DNA Marker, lane 1; pET 30-SQR restriction digested with NdeI-XhoI depicting a 5.44 kb pET30 Ec/Lic vector and a 1.2 kb Cpsqr gene insert, lane 2; Cp*sqr* gene PCR product, lane 3; pET30 Ec/Lic vector, lane 4. (B) The SDS-PAGE of SQR protein in recombinant *E. coli* BL21 cells with IPTG induction for 0, 3, and 6 h was show in lane 1-3, respectively; line 4 was protein molecular weight marker.

Fig. 2. The activity of SQR in recombinant *E. coli* BL21 cells. (A) The methylene blue spectrophotometric method for determining the sulfide biodegradation capability of *E. coli* BL21 cells expressing SQR protein. (B) a, b, and c are corresponded to the reactive state of 0, 2, and 4 min in Fig. 2A, respectively.

Fig. 3. SEM images of NPG before (A) and after (B) *E. coli* BL21 cells loading; The electrochemical reaction of *E. coli*/NPG/GCE bioelectrode (C).

Fig. 4. (A) CVs of NPG/GCE electrode and *E. coli*/NPG/GCE bioelectrode in deaerated PBS. (C) DPVs of NPG/GCE electrode, *E. coli*/NPG/GCE bioelectrode, HRP/NPG/GCE bioelectrode, and *E. coli*/HRP/NPG/GCE bioelectrode in deaerated PBS with 4 mM sulfide. CVs of *E. coli*/NPG/GCE bioelectrode at different scan rates ranging in deaerated PBS (B) and in deaerated PBS with 2 mM sulfide (D); The inset profiles show the peak current density as a function of the square root of scan rate.

Fig. 5. (A) The electrochemical response of the *E. coli*/NPG/GCE bioelectrode as a function of the sulfide concentration. The inset profiles show the calibration curve

between the peak current density and sulfide concentration (50 μM–5 mM). Effects of interferents on *E. coli*/NPG/GCE bioelectrode: (B) cations; (C) anions; (D) organic pollutants (Cat: catechol; DMSO: dimethyl sulfoxide; CA: carbazole); Content is the molar ratios of interferents to sulfide.

Fig. 1

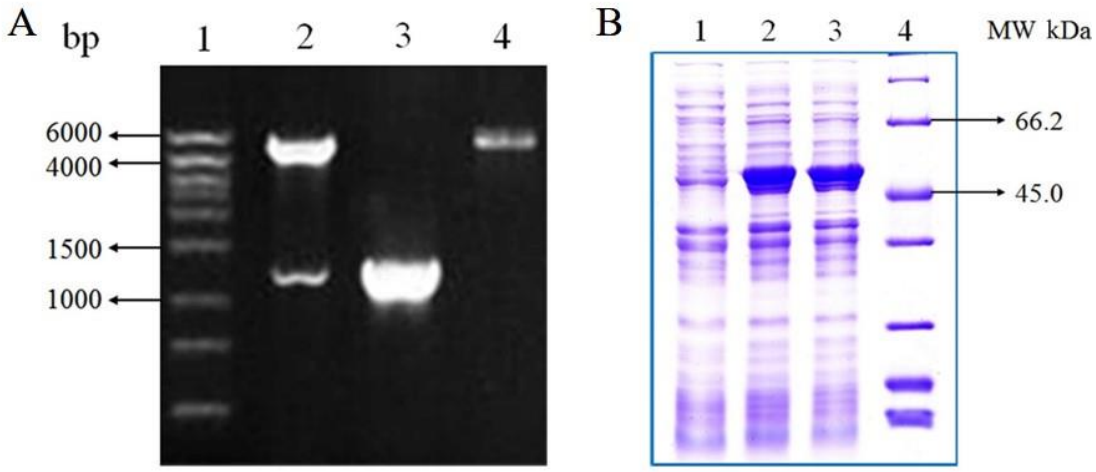

Fig. 2

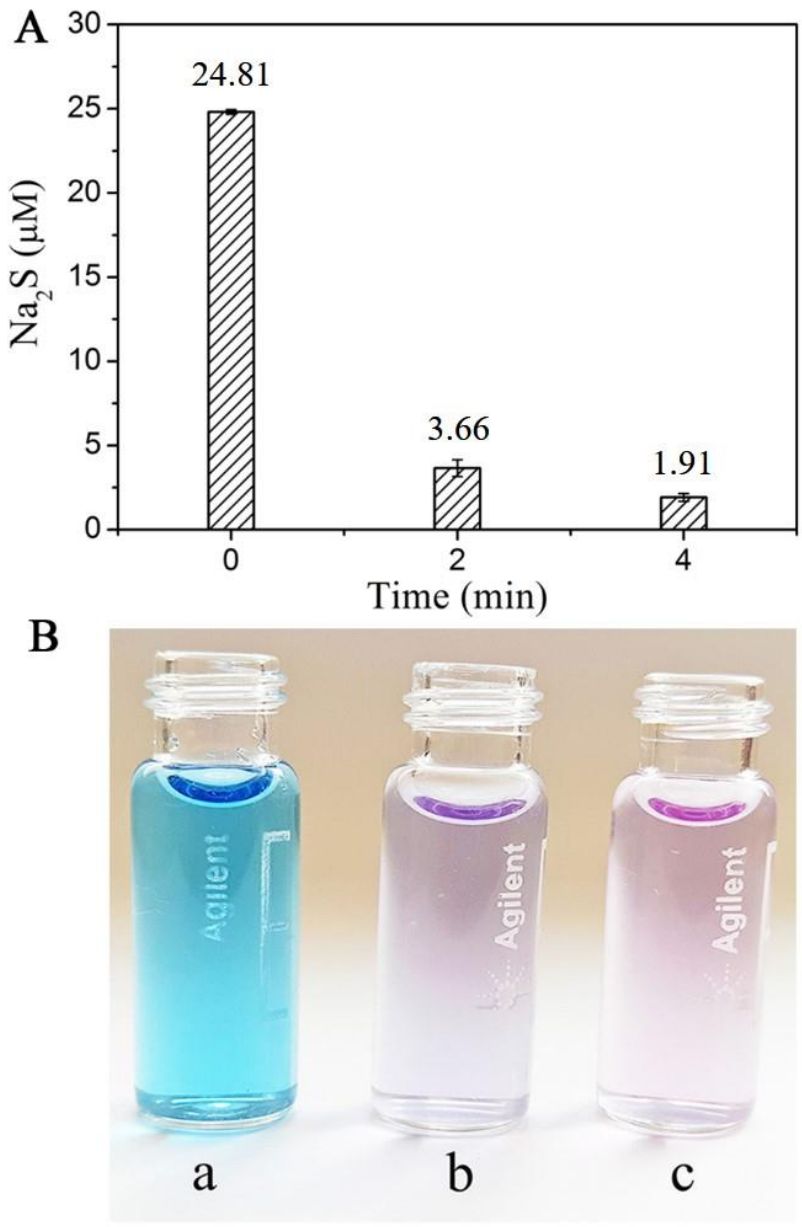
A
30
25
20
15
10
5
0
Na_2S (μM)
24.81
3.66
1.91
0
2
4
Time (min)
B
Agilent
Agilent
Agilent
a
b
c

Fig. 3

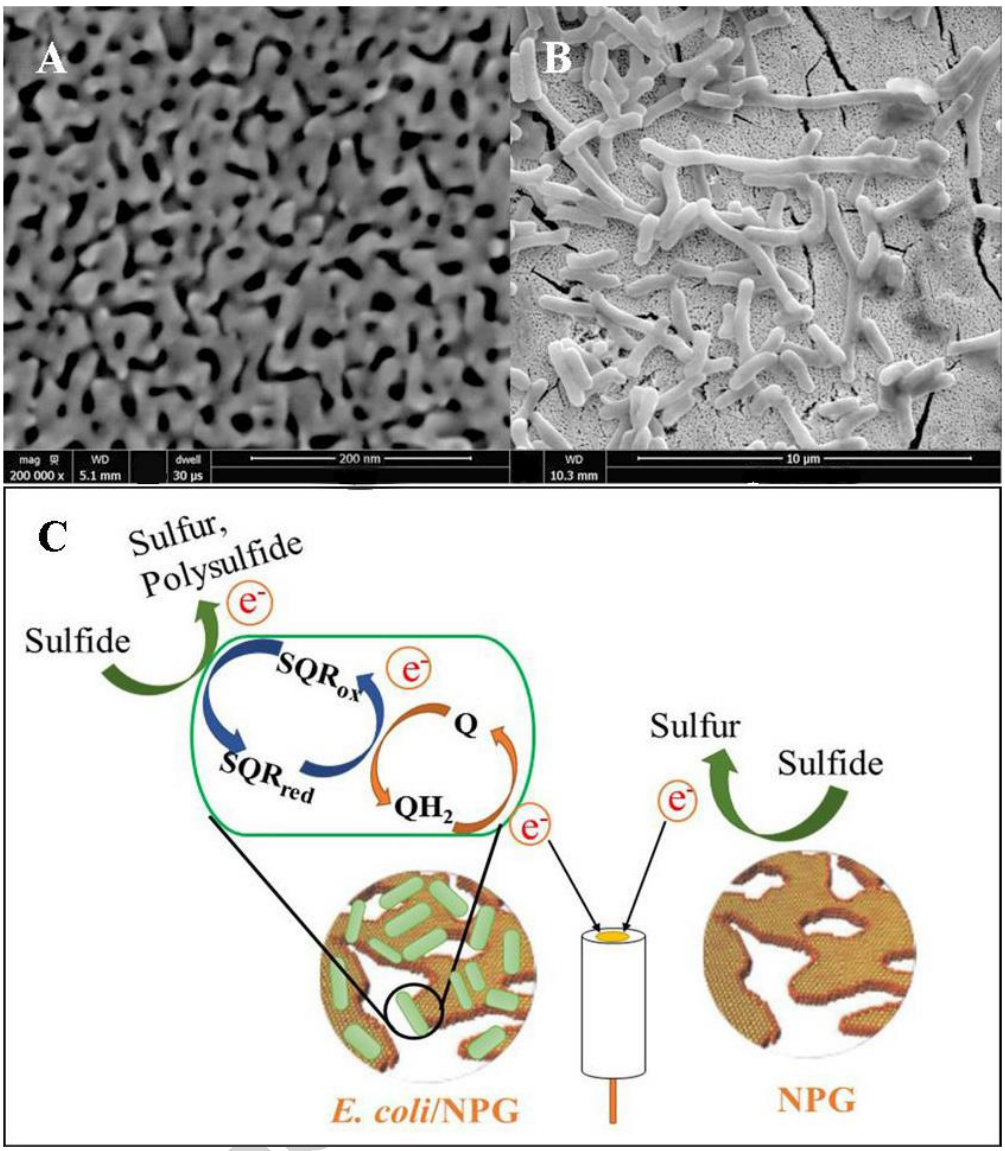
A
B
mag
200 000 x
WD
5.1 mm
dwell
30 µs
200 nm
WD
10.3 mm
10 µm
C
Sulfur,
Polysulfide
e-
Sulfide
SQRox
e-
Q
SQRred
QH2
e-
Sulfur
Sulfide
e-
E. coli/NPG
NPG

Fig. 4

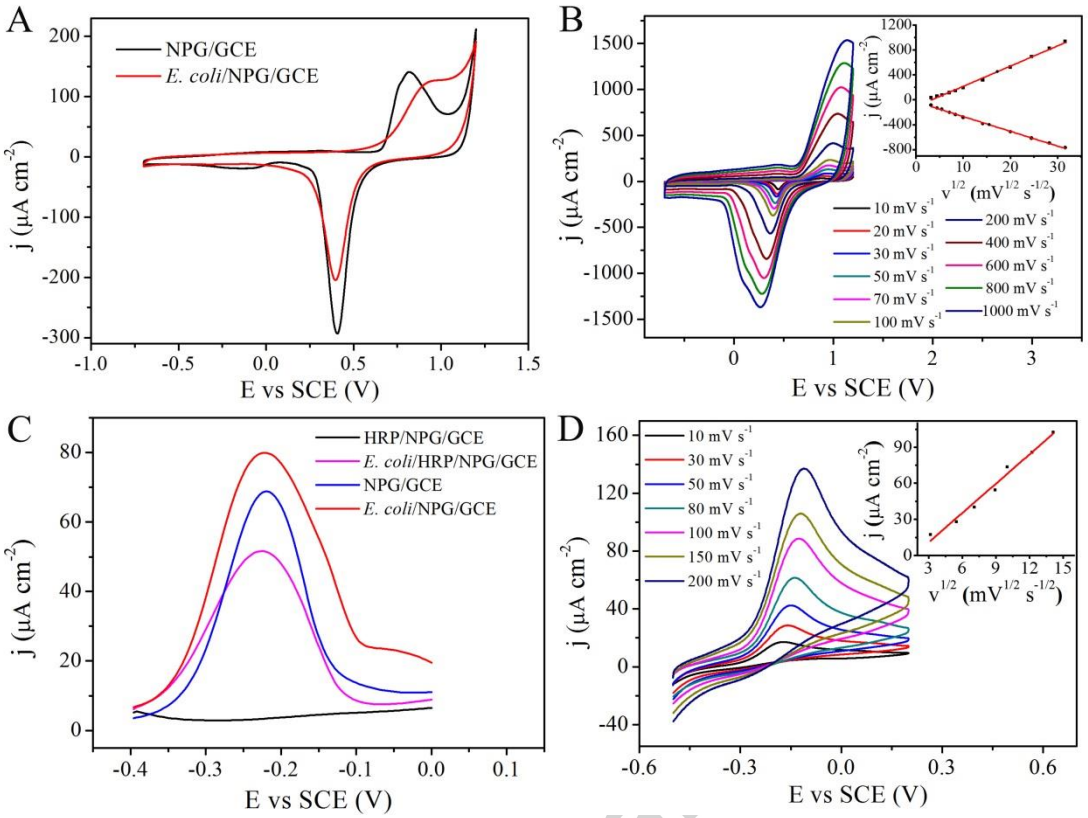

Fig. 5

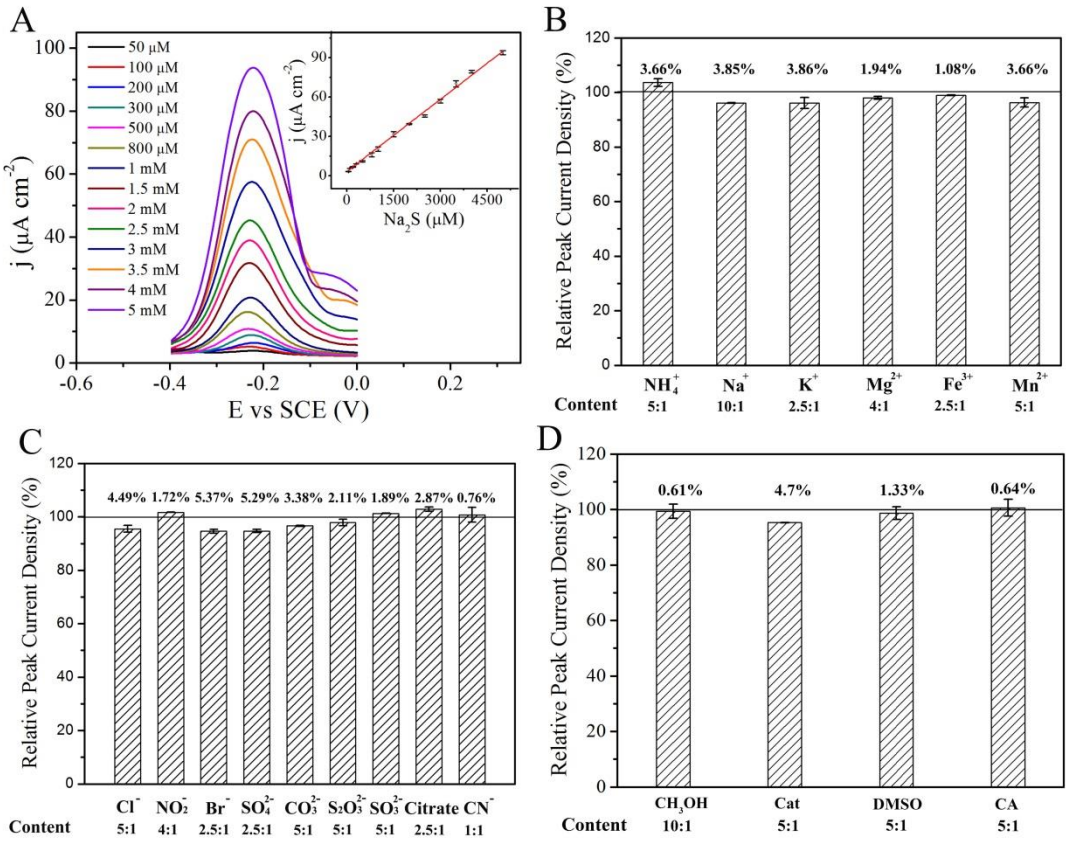

Highlights

► A novel microbial biosensor based on recombinant bacteria was developed for sulfide detection.

► The resulting microbial biosensor showed high sensitivity, anti-interference ability, and good stability.

► The microbial biosensor achieved reliable sulfide detection in wastewater.